

Calculations of parity nonconserving s - d transitions in Cs, Fr, Ba⁺, and Ra⁺

V.A. Dzuba, V.V. Flambaum, and J.S.M. Ginges

School of Physics, University of New South Wales, Sydney 2052, Australia

(October 22, 2018)

Abstract

We have performed *ab initio* mixed-states and sum-over-states calculations of parity nonconserving (PNC) electric dipole (E1) transition amplitudes between s - d electron states of Cs, Fr, Ba⁺, and Ra⁺. For the lower states of these atoms we have also calculated energies, E1 transition amplitudes, and lifetimes. We have shown that PNC E1 transition amplitudes between s - d states can be calculated to high accuracy. Contrary to the Cs $6s$ - $7s$ transition, in these transitions there are no strong cancelations between different terms in the sum-over-states approach. In fact, there is one dominating term which deviates from the sum by less than 20%. This term corresponds to an s - $p_{1/2}$ weak matrix element, which can be calculated to better than 1%, and a $p_{1/2}$ - $d_{3/2}$ E1 transition amplitude, which can be measured. Also, the s - d amplitudes are about four times larger than the corresponding s - s transitions. We have shown that by using a hybrid mixed-states/sum-over-states approach the accuracy of the calculations of PNC s - d amplitudes could compete with that of Cs $6s$ - $7s$ if $p_{1/2}$ - $d_{3/2}$ E1 amplitudes are measured to high accuracy.

PACS: 32.80.Ys,31.15.Ar

Typeset using REVTeX

I. INTRODUCTION

Precise low-energy experiments on parity nonconservation (PNC) in atoms provide a test of the standard model of elementary particle interactions. By measuring PNC electric dipole (E1) transition amplitudes, the value of the nuclear weak charge can be extracted by comparison with calculations. In a recent PNC experiment with cesium [1] the PNC E1 transition amplitude between the $6s$ and $7s$ states has been determined with an unprecedented accuracy of 0.35%. However, interpretation of the experiment is limited by the accuracy of the atomic calculations. Since 1989, calculations of the $6s$ - $7s$ transition in Cs have been at the 1% level [2,3]. At this level of accuracy the value of the nuclear weak charge is consistent with that predicted by the Standard Model. Recent measurements of values relevant to the PNC E1 amplitude (E1 transition amplitudes, hyperfine structure constants) are in much better agreement with the calculated values than they were ten years ago. From this it has been claimed that the accuracy of the calculated PNC E1 amplitude is 0.4% [4]. Re-interpreting the Cs measurement with the higher accuracy, while using the calculations [2,3], the value of the nuclear weak charge gives a 2.5σ deviation from the Standard Model prediction [4]. However, inclusion of the Breit interaction into the calculations reduces the deviation by about 1σ [5,6]. Note that these measurements give the best limits on new physics beyond the Standard Model, such as extra Z bosons, leptoquarks, composite fermions [7–9].

One obviously needs an independent confirmation of the Cs result. In this paper we show that the accuracy of calculations of PNC E1 transitions between s - d states of Cs, Fr, Ba⁺, and Ra⁺ could compete with that of the Cs $6s$ - $7s$ transition. The experiment for the $6s$ - $5d$ transition in Ba⁺ is already in progress [10].

II. MANY-BODY CALCULATIONS

We perform calculations for N -electron atoms with one external electron above closed shells. The calculations start from the relativistic Hartree-Fock (RHF) method in the \hat{V}^{N-1} approximation. The single-electron RHF Hamiltonian is

$$\hat{H}_0 = c\boldsymbol{\alpha} \cdot \hat{\mathbf{p}} + (\beta - 1)c^2 - Z/r + \hat{V}^{N-1}, \quad (1)$$

α and β are Dirac matrices and $\hat{\mathbf{p}}$ is the electron momentum. The accuracy of RHF energies is of the order of 10% for heavy atoms like Cs, Fr, Ba⁺, and Ra⁺.

In order to obtain more realistic wavefunctions, electron-electron correlations must be taken into account. Correlation corrections to the electron orbitals are calculated using the ‘‘correlation potential’’ method [11]. This method corresponds to adding a non-local correlation potential $\hat{\Sigma}$ to the potential \hat{V}^{N-1} in the RHF equation (1) and then solving for the states of the external electron. The correlation potential is defined such that its average value coincides with the correlation correction to energy, $\delta E_i = \langle \psi_i | \hat{\Sigma} | \psi_i \rangle$. The correlation potential is calculated by means of many-body perturbation theory in the residual Coulomb interaction

$$U = \hat{H} - \sum_{i=1}^N \hat{H}_0(\mathbf{r}_i) = \sum_{i < j}^N \frac{1}{|\mathbf{r}_i - \mathbf{r}_j|} - \sum_{i=1}^N \hat{V}^{N-1}(\mathbf{r}_i), \quad (2)$$

where \hat{H} is the exact Hamiltonian of an atom. The lowest-order correlation diagrams (second-order in U) are presented in Fig. 1. At this level of calculation the accuracy for energy levels is about 1%.

Using the correlation potential method and the Feynman diagram technique we include three series of higher order diagrams which are calculated in all orders of perturbation theory [2,12,13]. These are screening of the electron-electron interaction, the hole-particle interaction, and chaining of the self-energy operator $\hat{\Sigma}$. The electron-electron screening (see Fig. 2) and the hole-particle interaction (Fig. 3) are incorporated into the self-energy operator $\hat{\Sigma}$ (Fig. 4). Chaining of the self-energy operator to all orders (Fig. 5) is then calculated by adding $\hat{\Sigma}$ to the Hartree-Fock potential \hat{V}^{N-1} and solving the equation

$$(\hat{H}_0 + \hat{\Sigma} - \epsilon)\psi = 0 \quad (3)$$

iteratively for the states of the external electron. In this way “Brueckner” energies and orbitals are obtained. These energies have an accuracy of the order of 0.1%. The wavefunctions can be further modified by placing a coefficient before $\hat{\Sigma}$ such that the corresponding energy coincides with the experimental value. This fitting of the Brueckner orbitals can be considered as a way of including higher-order diagrams into the calculations.

We use the time-dependent Hartree-Fock method (which is equivalent to the random-phase approximation with exchange) to calculate the interaction of external fields with atomic electrons. In this paper we deal with two external fields: the electric field of the photon (E1 transition amplitudes) and the weak field of the nucleus. In the RHF approximation the interaction between an external field \hat{H}_{ext} and atomic electrons is $\langle \psi_1^{HF} | \hat{H}_{\text{ext}} | \psi_2^{HF} \rangle$, where ψ_1^{HF} and ψ_2^{HF} are RHF orbitals. Inclusion of the polarization of the atomic core by an external field is reduced to the addition of a correction $\delta\hat{V}$ (which is the correction to the Hartree-Fock potential due to the interaction between the core and the external field) to the operator which describes the interaction, $\langle \psi_1^{HF} | \hat{H}_{\text{ext}} + \delta\hat{V} | \psi_2^{HF} \rangle$. To include “Brueckner-type” correlation corrections the RHF orbitals are simply replaced by Brueckner ones, $\langle \psi_1^{Br} | \hat{H}_{\text{ext}} + \delta\hat{V} | \psi_2^{Br} \rangle$. The Brueckner-type correlations give the dominant corrections to the RHF approximation. They correspond to diagrams in which the interactions occur in the external lines of the self-energy operator (see, e.g., Fig. 6). Those diagrams in which the E1 interaction occurs in the internal lines are known as “structural radiation”, while those in which the weak interaction occurs in the internal lines are known as the “weak correlation potential” (see, e.g., Fig. 7). There is also a correction to the amplitudes arising from the normalization of states [11]. The structural radiation, weak correlation potential, and normalization contributions are suppressed by the small parameter $E_{\text{ext}}/E_{\text{core}} \sim 1/10$, where E_{ext} and E_{int} are excitation energies of the external and core electrons, respectively.

The nuclear spin-independent weak interaction of an electron with the nucleus is

$$\hat{H}_W = -\frac{G_F}{2\sqrt{2}}\rho(r)Q_W\gamma_5 \quad (4)$$

where G_F is the Fermi constant, Q_W is the weak charge of the nucleus, γ_5 is a Dirac matrix, and $\rho(r)$ is the density of the nucleus. Parity nonconserving E1 transition amplitudes, arising due to the simultaneous interaction of atomic electrons with the nuclear weak charge and the photon field, can be calculated using two methods: from a mixed-states approach; or from a sum-over-states approach, in which experimental values (energies and E1 transition

amplitudes) can be explicitly included. Contributions to PNC E1 transition amplitudes are presented diagrammatically in Figs. 6, 7.

In the mixed-states approach the PNC E1 transition amplitude between the states ns and $(n-1)d_{3/2}$, $n = 6$ for Cs and Ba⁺, $n = 7$ for Fr and Ra⁺, is given by

$$E1_{PNC} = \langle \psi_{(n-1)d} | \hat{H}_{E1} + \delta \hat{V}_{E1} | \delta \psi_{ns} \rangle + \langle \psi_{(n-1)d} | \hat{H}_W + \delta \hat{V}_W | \tilde{\psi}_{ns} \rangle + \langle \psi_{(n-1)d} | \delta \hat{V}_{E1W} | \psi_{ns} \rangle, \quad (5)$$

where $\delta \psi$ and $\delta \hat{V}_W$ are corrections to single-electron wavefunctions and the Hartree-Fock potential caused by the weak interaction, $\tilde{\psi}$ and $\delta \hat{V}_{E1}$ are corrections to wavefunctions and the Hartree-Fock potential caused by the electric field of the photon, $\delta \hat{V}_{E1W}$ is the correction to the core potential due to the simultaneous action of the weak field and the electric field of the photon; the wavefunctions $\psi_{(n-1)d}$ and ψ_{ns} correspond to Brueckner orbitals, and the corrections $\delta \psi$ and $\tilde{\psi}$ are found by solving the equations:

$$\begin{aligned} (\hat{H}_0 + \hat{\Sigma} - \epsilon) \delta \psi &= -(\hat{H}_W + \delta \hat{V}_W) \psi \\ (\hat{H}_0 + \hat{\Sigma} - \epsilon) \tilde{\psi} &= -(\hat{H}_{E1} + \delta \hat{V}_{E1}) \psi. \end{aligned}$$

This method is equivalent to calculating the diagrams presented in Fig. 6 (with $\hat{\Sigma}$ chained to all orders, Fig. 5) with the inclusion of the core polarization diagrams presented in Fig. 8.

Parity nonconserving E1 transition amplitudes between the states ns and $(n-1)d$ in the sum-over-states approach have the form

$$\begin{aligned} E1_{PNC} &= \sum_{n'} \frac{\langle (n-1)d_{3/2} | \hat{H}_{E1} + \delta \hat{V}_{E1} | n' p_{1/2} \rangle \langle n' p_{1/2} | \hat{H}_W + \delta \hat{V}_W | ns \rangle}{E_{ns} - E_{n' p_{1/2}}} \\ &+ \sum_{n'} \frac{\langle (n-1)d_{3/2} | \hat{H}_W + \delta \hat{V}_W | n' p_{3/2} \rangle \langle n' p_{3/2} | \hat{H}_{E1} + \delta \hat{V}_{E1} | ns \rangle}{E_{nd_{3/2}} - E_{n' p_{3/2}}}, \quad (6) \end{aligned}$$

where the sum is taken over a complete set of $p_{1/2}$ and $p_{3/2}$ states.

Note that the sum-over-states approach should also include the states with double-excitations like, for example in Cs, $\langle 5p^6 6s | \hat{H}_W | 5p^5 6p 7s \rangle$. In the mixed-states approach these states are included, for example, in the last term of Eq. 5 (see also diagram (c) of Fig. 8). These exotic states contribute due to their mixing with the single-excited electron states. This means that the mixed-states calculation (5) is more complete than the sum-over-states (6) *unless* the high-energy states with two or more excited electrons are included into the sum.

However, the accuracy of pure *ab initio* calculations for s - d transitions is not very good because of the huge correlations for d -states. On the other hand, we will see in the next section that this problem can be avoided in the sum-over-states approach by using experimental values for the p - d E1 transition amplitudes. Therefore, the best accuracy can be achieved when both methods are combined. Substitution of experimental values into the sum-over-states approach leads to a correction to the PNC amplitude which can be added to the mixed-states result. Following this procedure, it is possible to determine the PNC s - d amplitudes with an accuracy of about 1% (see discussion in the end of the next section).

III. RESULTS

Hartree-Fock energies for Cs, Fr, Ba⁺, and Ra⁺ are presented in Table I. These have an accuracy of the order of 10%. The Brueckner energies, including the three series of higher order diagrams, are also presented in Table I. These energies have an accuracy of the order of 0.1%.

Electric dipole transition amplitudes between the states m and m' are calculated in length form, $\langle m' | \hat{H}_{E1} | m \rangle = \langle m' | \mathbf{r} | m \rangle = C_{mm'} R$, where $C_{mm'}$ are angular coefficients and R is the radial integral. In Table II we present radial integrals relevant to the sum-over-states calculation for Cs, Fr, Ba⁺, and Ra⁺. In this table we present the values obtained in the RHF approximation and show the contribution of core polarization to the RHF integrals; we also present the (unfitted) Brueckner results and the contributions arising from structural radiation and normalization of states. In Table III we present radial integrals between the lower states of the four atoms which are calculated with fitted Brueckner orbitals and with structural radiation and normalization contributions included. Experimental values for Cs and Fr are presented in Table IV. The Cs transitions $5d_{3/2}-6p_{3/2}$ and $5d_{3/2}-6p_{1/2}$ were extracted from the measurement [26] of the $5d_{3/2}$ lifetime, $\tau = 909(15)$ ns by assuming that the ratio of the calculated radial integrals corresponds to the ratio of the experimental values. This assumption was also used to obtain the Fr $7d_{3/2}-7p_{3/2}$ and $7d_{3/2}-7p_{1/2}$ radial integrals from the measured lifetime $\tau = 73.6(3)$ ns [28]. With the exception of the Cs $6s-7p_{1/2}$ transition, the calculations of $s-p_{1/2}$ radial integrals agree with experiment at the level of 0.1%. The poor accuracy of the $6s-7p_{1/2}$ radial integral is due to the fact that the main RHF contribution is very small and the relative contribution of all corrections is large. The $5d-6p$ radial integrals for Cs have poor accuracy, deviating from experiment by about 4%. This is indicative of the poor calculation of d -states due to very large correlation corrections. The accuracy for the Fr $7d-7p$ radial integrals is about 1%. The reason that this accuracy is better than that for Cs $5d-6p$ is because the accuracy of the higher d -levels (here $7d$ rather than $6d$) is better due to smaller correlation corrections.

We have calculated the lifetimes of the low-lying states of Ba⁺ and Ra⁺. The $nd_{3/2}$ states of Ba⁺ ($n = 6$) and Ra⁺ ($n = 7$) decay directly to the ground state via the E2 transition; the $nd_{5/2}$ states decay via both the E2 and M1 transitions. Lifetimes of the Ba⁺ $5d$ states are presented in Table V. The calculations were performed with fitted Brueckner orbitals; core polarization, structural radiation, and normalization contributions were included into the E2 transition amplitudes. The calculations are in good agreement with experiment. We have also presented the calculations performed by Guet and Johnson [29]. It appears that for the state $5d_{5/2}$ they have not taken into account the M1 transition. This seems to be the reason for the discrepancy between the lifetime calculations for this state. From our calculations it is seen that inclusion of the M1 transition effectively decreases the lifetime of the $5d_{5/2}$ state from 36.3 s to 30.3 s. For Ra⁺ we obtained the lifetimes $\tau = 0.641$ s and $\tau = 0.302$ s for the states $6d_{3/2}$ and $6d_{5/2}$, respectively; these were calculated in the same way as for the Ba⁺ $5d$ states. The lifetimes for states of Ra⁺ have not been measured. Lifetimes of all other states are strongly dominated by E1 transitions and so can be calculated using the radial integrals presented in Table III. The calculated lifetimes of the $6p$ states of Ba⁺ are in excellent agreement with experiment and calculations by Guet and Johnson (see Table V).

The mixed-states results for the E1 PNC transition amplitudes are listed in Table VI.

The results of the sum-over-states calculation, and the contributions of the six terms corresponding to the summation of the $n-(n+2)$ p states, are presented in Table VII. In both calculations the contributions of structural radiation, weak correlation potential, and normalization of states are not included. The s - d PNC amplitudes are up to about four times as large as their corresponding s - s amplitudes. Furthermore, unlike the contributions to the sum-over-states calculation in Cs $6s$ - $7s$, in which the dominant contribution is about twice as large as the final result due to strong cancelations between three major terms in the sum, the PNC s - d transitions in Cs, Fr, Ba⁺, and Ra⁺ are strongly dominated by a single term. In each case this term corresponds to $\langle (n-1)d_{3/2} | \hat{H}_{E1} | np_{1/2} \rangle \langle np_{1/2} | \hat{H}_W | ns \rangle / (E_{ns} - E_{np_{1/2}})$; this term is different from the sum by less than 20%.

Because the Cs $6p_{1/2}$ - $5d_{3/2}$ E1 transition and energies are known we can correct the mixed-states PNC result. Replacing the calculated values by these experimental values in the dominating term of the sum (6) for Cs increases this term (and the total sum) by about 4%. This correction is mostly due to the difference between the calculated and experimental E1 amplitude (see Table IV). From the 1% accuracy of calculations of hyperfine structure constants for s and $p_{1/2}$ states [13] we can expect that the accuracy of the s - $p_{1/2}$ weak matrix elements in this calculation is also about 1%. Therefore, we can say that the uncertainty in the calculated *ab initio* s - d $E1_{PNC}$ amplitudes is dominated by the uncertainty of the p - d E1 matrix elements and constitutes about 4% for Cs and about the same value, or a little more, for other atoms.

The correction to the $6s$ - $5d$ $E1_{PNC}$ amplitude in Cs discussed in the previous paragraph is $0.126 \text{ } iea_B(-Q_W/N)$. When it is added to the mixed-states result, the new value is $E1_{PNC}(6s-5d) = 3.75 \text{ } iea_B(-Q_W/N)$. Since using the experimental $6p$ - $5d$ E1 amplitude removes the main source of uncertainty, the accuracy of the modified result must be considerably better than 4%. Assuming high accuracy of p - d transition amplitudes, one can say that the uncertainty is now dominated by the uncertainty of calculated s - p weak matrix elements which is about 1% (however, we believe that this accuracy can be improved beyond 1% with the inclusion of weak correlation potential and normalization contributions). More rigorous calculations and a more detailed analysis of the accuracy will be carried out when the need arises from the progress in experiments. We expect that calculations of $E1_{PNC}$ amplitudes for Cs, Fr, Ba⁺, and Ra⁺, with empirical corrections, can reach an accuracy of about 1%.

IV. CONCLUSION

We have calculated the PNC E1 transition amplitudes between s - d states of Cs, Fr, Ba⁺, and Ra⁺. Generally, high accuracy cannot be reached in purely *ab initio* calculations of these transitions due to the poor accuracy of d -states. However, we have shown from a sum-over-states calculation that, unlike the Cs $6s$ - $7s$ transition, the s - d transitions we have mentioned are strongly dominated by a single term in the sum. Moreover, this term corresponds to an s - $p_{1/2}$ weak matrix element, which can be calculated with an accuracy of better than 1%, and a $p_{1/2}$ - $d_{3/2}$ E1 transition amplitude, which can be taken from experiment. The need to reach high accuracy for d states is therefore avoided. In addition to this, PNC s - d transitions are larger than the corresponding s - s transitions. The mixed-states calculation can be modified by correcting the terms in the sum-over-states by inserting experimental E1 transitions and

energies. If $p_{1/2}$ - $d_{3/2}$ E1 transition amplitudes are measured to high accuracy, we believe that the accuracy of the calculations of s - d PNC transitions for Cs, Fr, Ba⁺, and Ra⁺ can reach 1%.

ACKNOWLEDGMENTS

We are grateful to N. Fortson for useful discussions. This work was supported by the Australian Research Council.

REFERENCES

- [1] C.S. Wood, S.C. Bennett, D. Cho, B.P. Masterson, J.L. Roberto, C.E. Tanner, and C.E. Wieman, *Science* **275**, 1759 (1997).
- [2] V.A. Dzuba, V.V. Flambaum, and O.P. Sushkov, *Phys. Lett. A* **141**, 147 (1989).
- [3] S.A. Blundell, W.R. Johnson, and J. Sapirstein, *Phys. Rev. Lett.* **65**, 1411 (1990); *Phys. Rev. D* **45**, 1602 (1992).
- [4] S.C. Bennett and C.E. Wieman, *Phys. Rev. Lett.* **82**, 2484 (1999); **82**, 4153 (1999); **83**, 889 (1999).
- [5] A. Derevianko, *Phys. Rev. Lett.* **85**, 1618 (2000).
- [6] V.A. Dzuba, C. Harabati, W.R. Johnson, and M.S. Safronova; submitted to *Phys. Rev. A*.
- [7] R. Casalbuoni, S. De Curtis, D. Dominici, and R. Gatto, *Phys. Lett. B* **460**, 135 (1999).
- [8] J.L. Rosner, *Phys. Rev. D* **61**, 016006 (1999).
- [9] J. Erler and P. Langacker, *Phys. Rev. Lett.* **84**, 212 (2000).
- [10] N. Fortson, *Phys. Rev. Lett.* **70**, 2383 (1993); private communication.
- [11] V.A. Dzuba, V.V. Flambaum, P.G. Silvestrov, and O.P. Sushkov, *J. Phys. B* **20**, 1399 (1987).
- [12] V.A. Dzuba, V.V. Flambaum, and O.P. Sushkov, *Phys. Lett. A* **140**, 493 (1989).
- [13] V.A. Dzuba, V.V. Flambaum, A.Ya. Kraftmakher, and O.P. Sushkov, *Phys. Lett. A* **142**, 373 (1989).
- [14] C.E. Moore, *Atomic Energy Levels*, Natl. Bur. Stand. Ref. Data Ser., Natl. Bur. Stand. (U.S.) Circ. No. 35 (U.S. GPO, Washington, D.C., 1971), Vol. III.
- [15] J. Bauche *et al*, *J. Phys. B* **19**, L593 (1986).
- [16] H.T. Duong *et al*, *Europhys. Lett.* **3**, 175 (1987).
- [17] S.V. Andreev, V.S. Letokhov, and V.I. Mishin, *Phys. Rev. Lett.* **59**, 1274 (1987); S.V. Andreev, V.I. Mishin, and V.S. Letokhov, *J. Opt. Soc. Am. B* **5**, 2190 (1988).
- [18] E. Arnold *et al*, *J. Phys. B* **23**, 3511 (1990).
- [19] J.E. Simsarian, W. Shi, L.A. Orozco, G.D. Sprouse, and W.Z. Zhao, *Opt. Lett.* **21**, 1939 (1996).
- [20] J.E. Simsarian, W.Z. Zhao, L.A. Orozco, and G.D. Sprouse, *Phys. Rev. A* **59**, 195 (1999).
- [21] J.M. Grossman *et al*, *Phys. Rev. A* **62**, 052507 (2000).
- [22] R.J. Rafac, C.E. Tanner, A.E. Livingston, and H.G. Berry, *Phys. Rev. A* **60**, 3648 (1999).
- [23] L.N. Shabanova, Yu. M. Monakov, and A.M. Khlustalov, *Opt. Spektrosk.* **47**, 3 (1979).
- [24] M.-A. Bouchiat, J. Guena, and L. Pottier, *J. Phys. (Paris) Lett.* **45**, L523 (1984).
- [25] S. C. Bennett, J. L. Roberts, and C. E. Wieman, *Phys. Rev. A* **59**, R16 (1999).
- [26] D. DiBerardino, C.E. Tanner, and A. Sieradzian, *Phys. Rev. A* **57**, 4204 (1998).
- [27] J.E. Simsarian, L.A. Orozco, G.D. Sprouse, and W.Z. Zhao, *Phys. Rev. A* **57**, 2448 (1998).
- [28] J.M. Grossman *et al*, *Phys. Rev. A* **62**, 062502 (2000).
- [29] C. Guet and W.R. Johnson, *Phys. Rev. A* **44**, 1531 (1991).
- [30] E.H. Pinnington, R.W. Berends, and M. Lumsden, *J. Phys. B* **28**, 2095 (1995).
- [31] N. Yu, W. Nagourney, and H. Dehmelt, *Phys. Rev. Lett.* **78**, 4898 (1997).
- [32] A.A. Madej and J.D. Sankey, *Phys. Rev. A* **41**, 2621 (1990).

TABLES

TABLE I. Energy levels (ionization potentials) of the lower states of Cs, Fr, Ba⁺ and Ra⁺ in units $-\text{cm}^{-1}$.

State	Cs			Ba ⁺		
	RHF	Brueckner	Experiment ^a	RHF	Brueckner	Experiment ^a
6s	27954	31420	31407	75339	80813	80687
7s	12112	12851	12871	36852	38333	38332
8s	6793	7082	7090	22023	22651	22662
6p _{1/2}	18790	20275	20228	57265	60581	60425
7p _{1/2}	9223	9643	9641	30240	31332	31297
8p _{1/2}	5513	5701	5698	18848	19378	19351
6p _{3/2}	18389	19708	19674	55873	58860	58734
7p _{3/2}	9079	9460	9460	29699	30704	30676
8p _{3/2}	5446	5618	5615	18580	19075	19051
5d _{3/2}	14138	17023	16907	68139	76402	75813
6d _{3/2}	7920	8824	8818	33266	34740	34737
7d _{3/2}	4965	5362	5359	20251	20871	20887
5d _{5/2}	14163	16915	16810	67665	75525	75012
6d _{5/2}	7921	8781	8775	33093	34536	34532
7d _{5/2}	4963	5341	5338	20167	20777	20792
State	Fr			Ra ⁺		
	RHF	Brueckner	Experiment ^b	RHF	Brueckner	Experiment ^a
7s	28768	32841	32849	75900	81960	81842
8s	12282	13071	13116	36861	38405	38437
9s	6858	7164	7178	22004	22659	22677
7p _{1/2}	18856	20674	20612	56879	60681	60491
8p _{1/2}	9240	9730	9736	30053	31244	31236
9p _{1/2}	5521	5737	-	18748	19332	-
7p _{3/2}	17656	18944	18925	52906	55734	55633
8p _{3/2}	8811	9180	9191	28502	29447	29450
9p _{3/2}	5319	5486	-	17975	18462	18432
6d _{3/2}	13826	16610	-	62356	70149	69758
7d _{3/2}	7725	8583	8604	31575	33060	33098
8d _{3/2}	4857	5241	5248	19451	20079	20107
6d _{5/2}	13925	16413	-	61592	68449	68099
7d _{5/2}	7747	8496	8516	31204	32569	32602
8d _{5/2}	4863	5197	5203	19261	19849	19868

^aTaken from [14].

^bMeasured in Refs. [15–21].

TABLE II. Calculated radial integrals (a.u.) for Cs, Fr, Ba⁺, Ra⁺. We present RHF values, RHF with core polarization, the Brueckner result with core polarization included, and structural radiation and normalization of states; 0.0 signifies that the value is smaller than the number of figures specified.

Atom	Transition	RHF	RHF + core polar- ization	Brueckner + core polar- ization	Structural radiation	Normal- ization of states
Cs	$6s_{1/2} - 6p_{3/2}$	-6.432	-6.074	-5.500	-0.028	0.047
	$6s_{1/2} - 7p_{3/2}$	-0.602	-0.440	-0.463	-0.013	0.003
	$6s_{1/2} - 8p_{3/2}$	-0.245	-0.143	-0.162	-0.008	0.001
	$6p_{1/2} - 5d_{3/2}$	7.775	7.481	6.050	0.026	-0.050
	$7p_{1/2} - 5d_{3/2}$	-3.498	-3.591	-1.742	0.011	0.011
	$8p_{1/2} - 5d_{3/2}$	-0.860	-0.916	-0.556	0.007	0.003
Fr	$7s_{1/2} - 7p_{3/2}$	-6.140	-5.739	-5.128	-0.032	0.051
	$7s_{1/2} - 8p_{3/2}$	-0.949	-0.760	-0.748	-0.015	0.006
	$7s_{1/2} - 9p_{3/2}$	-0.452	-0.332	-0.336	-0.009	0.003
	$7p_{1/2} - 6d_{3/2}$	7.986	7.613	6.256	0.035	-0.061
	$8p_{1/2} - 6d_{3/2}$	-4.005	-4.116	-2.249	0.014	0.015
	$9p_{1/2} - 6d_{3/2}$	-0.941	-1.008	-0.704	0.008	0.004
Ba ⁺	$6s_{1/2} - 6p_{3/2}$	-4.744	-4.314	-4.056	-0.032	0.046
	$6s_{1/2} - 7p_{3/2}$	-0.226	-0.036	-0.015	-0.013	0.0
	$6s_{1/2} - 8p_{3/2}$	-0.068	0.054	0.076	-0.007	-0.001
	$6p_{1/2} - 5d_{3/2}$	3.244	2.964	2.634	0.026	-0.034
	$7p_{1/2} - 5d_{3/2}$	0.304	0.184	0.225	0.010	-0.002
	$8p_{1/2} - 5d_{3/2}$	0.169	0.092	0.099	0.007	-0.001
Ra ⁺	$7s_{1/2} - 7p_{3/2}$	-4.624	-4.154	-3.885	-0.035	0.048
	$7s_{1/2} - 8p_{3/2}$	-0.541	-0.320	-0.286	-0.015	0.003
	$7s_{1/2} - 9p_{3/2}$	-0.243	-0.098	-0.067	-0.009	0.001
	$7p_{1/2} - 6d_{3/2}$	3.851	3.448	3.067	0.037	-0.047
	$8p_{1/2} - 6d_{3/2}$	0.091	-0.075	0.009	0.014	0.0
	$9p_{1/2} - 6d_{3/2}$	0.075	-0.030	-0.014	0.008	0.0

TABLE III. Radial integrals (a.u.) for states of Cs, Fr, Ba⁺ and Ra⁺. Fitted Brueckner orbitals are used; core polarization, and structural radiation and normalization of states are also included.

		$6p_{1/2}$	$7p_{1/2}$	$8p_{1/2}$	$6p_{3/2}$	$7p_{3/2}$	$8p_{3/2}$
Cs	$6s$	-5.508	-0.313	-0.081	-5.482	-0.471	-0.171
	$7s$	5.211	-12.605	-1.137	5.625	-12.383	-1.419
	$8s$	1.266	11.386	-21.753	1.273	12.163	-21.252
	$5d_{3/2}$	6.072	-1.785	-0.560	6.120	-1.579	-0.506
	$6d_{3/2}$	-3.696	15.558	-4.234	-4.082	15.612	-3.726
	$7d_{3/2}$	-1.806	-5.632	27.670	-1.918	-6.379	27.773
	$5d_{5/2}$	-	-	-	6.190	-1.641	-0.522
	$6d_{5/2}$	-	-	-	-3.986	15.699	-3.886
	$7d_{5/2}$	-	-	-	-1.893	-6.186	27.876
Ba ⁺	$6s$	-4.054	0.121	0.141	-4.048	-0.030	0.063
	$7s$	3.053	-8.583	-0.139	3.362	-8.464	-0.401
	$8s$	0.863	6.080	-14.153	0.888	6.634	-13.884
	$5d_{3/2}$	2.646	0.226	0.103	2.584	0.285	0.135
	$6d_{3/2}$	-4.234	7.488	0.101	-4.520	7.311	0.282
	$7d_{3/2}$	-1.189	-7.134	13.494	-1.170	-7.674	13.195
	$5d_{5/2}$	-	-	-	2.658	0.279	0.133
	$6d_{5/2}$	-	-	-	-4.469	7.418	0.235
	$7d_{5/2}$	-	-	-	-1.1865	-7.5570	13.352
		$7p_{1/2}$	$8p_{1/2}$	$9p_{1/2}$	$7p_{3/2}$	$8p_{3/2}$	$9p_{3/2}$
Fr	$7s$	-5.242	-0.331	-0.093	-5.107	-0.748	-0.343
	$8s$	5.217	-12.326	-1.206	6.484	-11.536	-1.947
	$9s$	1.256	11.428	-21.382	1.215	13.777	-19.660
	$6d_{3/2}$	6.237	-2.229	-0.691	6.417	-1.553	-0.516
	$7d_{3/2}$	-3.014	15.893	-5.488	-4.186	16.175	-3.829
	$8d_{3/2}$	-1.606	-4.296	27.952	-1.975	-6.546	28.464
	$6d_{5/2}$	-	-	-	6.576	-1.684	-0.549
	$7d_{5/2}$	-	-	-	-3.974	16.368	-4.184
	$8d_{5/2}$	-	-	-	-1.917	-6.106	28.695
Ra ⁺	$7s$	-3.948	0.108	0.142	-3.877	-0.294	-0.082
	$8s$	3.104	-8.523	-0.168	4.038	-8.071	-0.891
	$9s$	0.867	6.167	-14.122	0.897	7.825	-13.137
	$6d_{3/2}$	3.074	0.011	-0.011	2.913	0.245	0.110
	$7d_{3/2}$	-3.774	8.262	-0.412	-4.662	7.801	0.256
	$8d_{3/2}$	-1.240	-6.152	14.649	-1.242	-7.812	13.854
	$6d_{5/2}$	-	-	-	3.109	0.224	0.105
	$7d_{5/2}$	-	-	-	-4.515	8.087	0.117
	$8d_{5/2}$	-	-	-	-1.281	-7.476	14.276

TABLE IV. Calculated (Table III) and experimental radial integrals (a.u.).

Atom	Transition	Calc.	Exp.
Cs	$6s-6p_{1/2}$	-5.508	-5.497(8) ^a
	$6s-6p_{3/2}$	-5.482	-5.476(6) ^a
	$6s-7p_{1/2}$	-0.313	-0.348(3) ^b
	$7s-6p_{1/2}$	5.211	5.185(27) ^c
	$7s-6p_{3/2}$	5.625	5.611(27) ^c
	$7s-7p_{1/2}$	-12.605	-12.625(18) ^d
	$7s-7p_{3/2}$	-12.383	-12.401(17) ^d
	$5d_{3/2}-6p_{1/2}$	6.072	6.31(5) ^e
	$5d_{3/2}-6p_{3/2}$	6.120	6.36(5) ^e
	$5d_{5/2}-6p_{3/2}$	6.190	6.40(2) ^e
Fr	$7s-7p_{1/2}$	-5.242	-5.238(10) ^f
	$7s-7p_{3/2}$	-5.107	-5.108(13) ^f
	$7d_{3/2}-7p_{1/2}$	-3.014	-3.05(1) ^g
	$7d_{3/2}-7p_{3/2}$	-4.186	-4.24(2) ^g
	$7d_{5/2}-7p_{3/2}$	-3.974	-4.02(8) ^g

^aReference [22].

^bReference [23].

^cReference [24].

^dReference [25].

^eReference [26].

^fReference [27].

^gReference [28].

 TABLE V. Lifetimes of low-lying states of Ba⁺.

Atom	State	$\tau^{\text{this work}}$	τ^{a}	τ^{expt}
Ba ⁺	$6p_{1/2}$	7.89 ns	7.99 ns	7.90(10) ns ^b
	$6p_{3/2}$	6.30 ns	6.39 ns	6.32(10) ns ^b
	$5d_{3/2}$	81.5 s	83.7 s	79.8(4.6) s ^c
	$5d_{5/2}$	30.3 s	37.2 s	34.5(3.5) s ^d

^aReference [29].

^bReference [30].

^cReference [31].

^dReference [32].

TABLE VI. Mixed-states results for PNC E1 transition amplitudes between the states $ns-(n-1)d$, $\langle(n-1)d|E1_z|ns\rangle$, where $n = 6$ for Cs and Ba^+ and $n = 7$ for Fr and Ra^+ ; units are $10^{-11}iea_B(-Q_W/N)$.

	Cs	Fr	Ba^+	Ra^+
Mixed-states $E1_{PNC}$	3.62	57.1	2.17	42.9

TABLE VII. Results of the sum-over-states calculations for the PNC E1 transition amplitudes for Cs, Fr, Ba^+ , and Ra^+ . We present the contributions of the terms in the sum corresponding to the intermediate $n-(n+2)p$ states, the contribution due to all other intermediate p -states, and the total value; units $10^{-11}iea_B(-Q_W/N)$; 0.0 means that the term is smaller than the number of figures specified.

		$\frac{\langle d \hat{H}_{E1} np_{1/2}\rangle\langle np_{1/2} \hat{H}_W s\rangle}{E_s-E_{np_{1/2}}}$	$\frac{\langle d \hat{H}_W np_{3/2}\rangle\langle np_{3/2} \hat{H}_{E1} s\rangle}{E_d-E_{np_{3/2}}}$
Cs	n=6	3.154	0.728
	n=7	-0.258	-0.013
	n=8	-0.047	-0.002
	Other		0.197
	Total		3.76
Fr	n=7	59.78	5.19
	n=8	-6.13	-0.15
	n=9	-1.10	-0.03
	Other		1.95
	Total		59.5
Ba^+	n=6	2.036	-0.264
	n=7	0.045	-0.001
	n=8	0.012	0.0
	Other		0.511
	Total		2.34
Ra^+	n=7	40.69	-2.33
	n=8	0.11	-0.05
	n=9	0.02	-0.01
	Other		7.47
	Total		45.9

FIGURES



FIG. 1. Second-order correlation diagrams for the valence electron ($\hat{\Sigma}$ operator). Dashed line is the Coulomb interaction. Loop is the polarization of the atomic core.



FIG. 2. Screening of the Coulomb interaction.

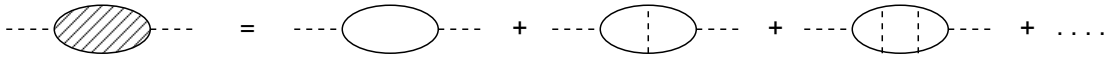


FIG. 3. Hole-particle interaction in the polarization operator.

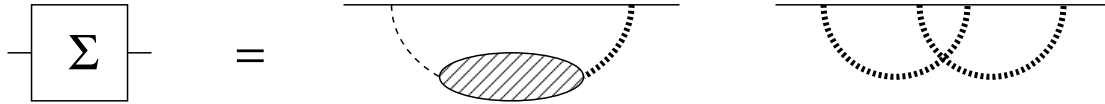


FIG. 4. The electron self-energy operator with screening and hole-particle interaction included.

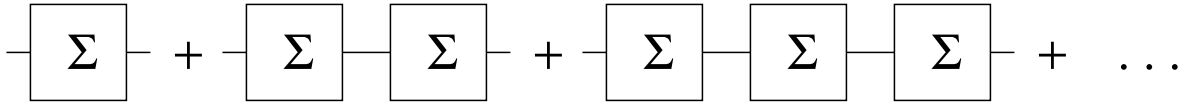


FIG. 5. Chaining of the self-energy operator.

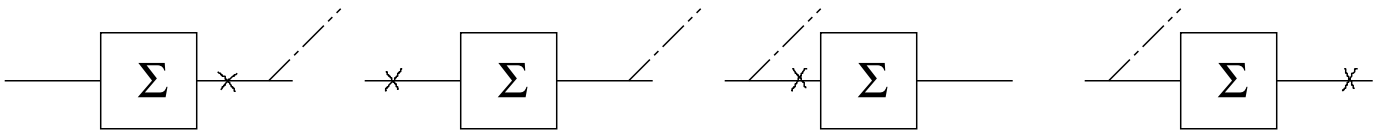


FIG. 6. Brueckner-type correlation corrections to the PNC E1 transition amplitude; the crosses denote the weak interaction and the dashed lines denote the electromagnetic interaction.

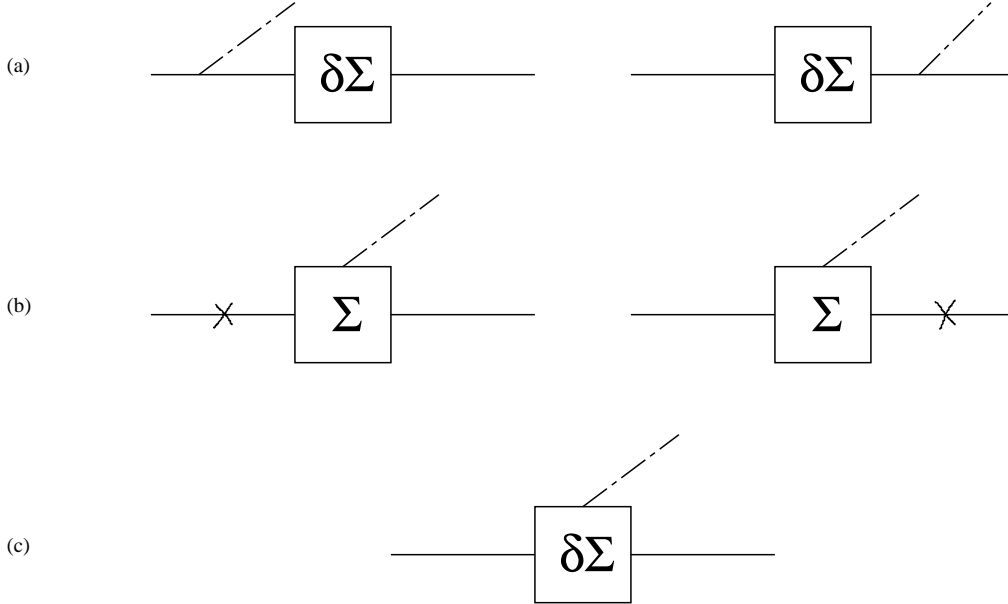


FIG. 7. Small corrections to the PNC E1 transition amplitude: external field inside the correlation potential. In diagrams (a) the weak interaction is inside the correlation potential ($\delta\Sigma$ denotes the change in Σ due to the weak interaction); this is known as the weak correlation potential. Diagrams (b,c) represent structural radiation (photon field inside the correlation potential). In diagram (b) the weak interaction occurs in the external lines; in diagram (c) both the weak and electromagnetic interactions occur in the internal lines.

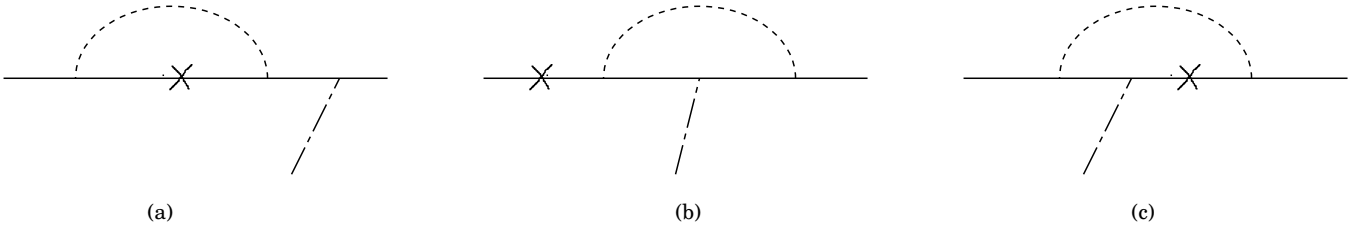


FIG. 8. Examples of diagrams representing the polarization of the atomic core by external fields. (The diagrams we have presented are exchange diagrams; there are also direct diagrams.) In diagrams (a) and (b) the core is polarized by a single field (the dashed line denotes the E1 interaction and the cross denotes the weak interaction). Diagram (c) corresponds to the polarization of the core by both fields.